Kevin J. Parker, Ph.D.
Robert M. Lerner, M.D., Ph.D.
Robert C. Waag, Ph.D.

Attenuation of Ultrasound: Magnitude and Frequency Dependence for Tissue Characterization[1]

Backscattered ultrasonic waveforms from selected regions of the liver were collected from B-scans of 11 male patients ranging from 13 to 41 years of age and analyzed to determine local values of both the magnitude and frequency dependence of attenuation. Processing was based on frequency domain analysis and also incorporated precise corrections for time-varying gain, nonlinear amplifier compression, and beam diffraction, which would otherwise degrade accuracy. The results demonstrate that (*a*) consistent and reproducible measurements of attenuation from one scan to the next are possible within a given patient, and (*b*) frequency dependence can deviate significantly from the linear relationship between frequency and attenuation commonly assumed for soft tissue. Based on the accuracy of the overall analysis and the reproducibility of the results, the authors suggest that a multivariate approach to clinical tissue characterization using both the magnitude and frequency dependence of ultrasonic attenuation may be possible.

Index terms: Liver, ultrasound studies, 761.1298 • Ultrasound, experimental • Ultrasound, physics • Ultrasound, tissue characterization, 761.91

Radiology 1984; 153: 785–788

LABORATORY studies have demonstrated that ultrasonic attenuation in tissue is affected by some disease processes: for example, infarcted myocardium shows a dramatic increase in attenuation at diagnostic frequencies (1, 2). However, because of the complexities of measuring attenuation of deep-lying organs *in vivo*, the diagnostic potential of such measurements remains largely unexploited. We have developed a technique for measuring the magnitude of tissue attenuation at discrete frequencies with a B-scan imager and using these data to assess frequency dependence (3). This is different from other methods that assume attenuation increases linearly with frequency and then seek to determine the attenuation "slope" (4–6), which has the disadvantage of constraining frequency dependence to a linear form which may not characterize abnormal tissues. Also, it has been shown that when frequency dependence is assumed to be linear, even small deviations can produce significant errors in attenuation calculations (7). In contrast, our more general technique has provided accurate measurements of complex materials where attenuation does not increase linearly with frequency (3).

MATERIALS AND METHODS

Two parasagittal abdominal scans 10–20 mm apart were obtained from each of 11 male volunteers 13 to 41 years of age who had given informed consent. Ten subjects were non-obese, in good general health, and had no history of any conditions affecting the liver. A 13-year-old boy with a 6-cm hepatic lesion, proven pathologically to be focal nodular hyperplasia, was also included in the study.

Waveforms from the liver were collected using an Octoson[2] B-scan imager with a usable bandwidth of 1 MHz centered around 2.5 MHz. Radiofrequency (RF) signals were digitized at a 10-MHz sampling rate and stored along with positional information and time-varying gain settings employed during data acquisition. Regions of interest were selected from the scan, focusing on homogeneous areas of uniform illumination and speckle density which were free from large specular reflectors and artifacts such as rib shadowing or reverberations, and the corresponding waveforms were isolated for further analysis. Between 80 and 128 waveforms each containing 750 digitized RF samples were used, representing an area measuring approximately 4 × 5 cm in the sagittal plane (Fig. 1).

Processing was performed as described elsewhere (3). Briefly, a computer-generated table listing the input and output characteristics of the Octoson was used to eliminate the effects of amplifier compression and time-varying gain from the signal, after which the corrected waveforms were segmented according to depth using Blackman windows (8) 100 sample points in length. A 50-point segmental overlap was employed; however, because of the shape of the window, correlation between adjacent segments was less than 10%. Fourier transforms were performed on the segments, and the ensemble averaged signal, which was proportional to the average acoustic pressure, was determined at each resolvable frequency as a function of depth. Curves of pressure *vs.* depth were then obtained and corrected for beam focusing or diffraction. Diffraction corrections were determined experimentally

---

[1] From the Departments of Electrical Engineering (K.J.P., R.C.W.) and Radiology (R.M.L., R.C.W.), University of Rochester, Rochester, N.Y. Received Feb. 9, 1984; accepted and revision requested April 23; revision received June 1.

This work was supported in part by grants from the Whitaker Foundation and the National Science Foundation.

[2] Ausonics, Inc., New Berlin, Wisc.

Figure 1

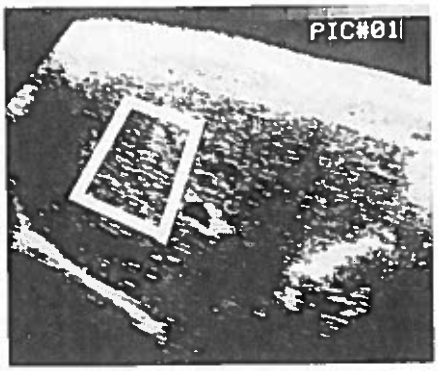

Abdominal sonogram with a superimposed rectangle indicating the region of interest within the liver.

TABLE I: Attenuation Power Law Parameters for the Liver in 11 male Subjects*

CASE	Age (yr.)	α_0(dB/cm-MHz^n)	n	α/f(dB/cm-MHz) at 3.0 MHz
I.	23	0.44	1.21	0.56
II.	29	0.51	0.97	0.49
III.	41	0.38	1.14	0.44
IV.	25	0.58	0.81	0.47
V.	29	0.47	0.91	0.43
VI.	26	0.45	0.97	0.44
VII.	22	0.57	0.83	0.48
VIII.	24	0.58	0.84	0.49
Mean of above data	27.3	0.497	0.96	0.48
IX.	33	0.88	0.56	0.54
X.	28	1.05	0.60	0.68
XI.	13	0.33	1.46	0.55

* Power law equation: $\alpha = \alpha_0 f^n$

Figure 2

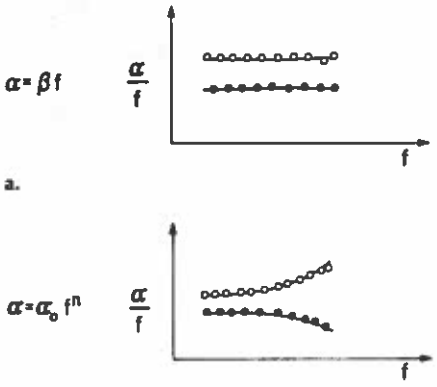

Graphs of normalized attenuation *vs.* frequency, showing hypothetical curves representing results from separate tissues with high and low values of attenuation.

a. When attenuation increases linearly with frequency, the slope of the curve is horizontal.

b. When the relationship between attenuation and frequency follows a more general power law, the curve slopes upward or downward depending on the value of n.

Figure 3

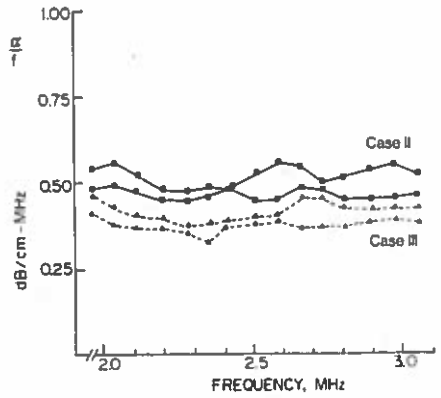

Measured values of attenuation ÷ frequency for two normal subjects. Each subject is represented by two curves derived from a pair of scans taken 10–20 mm apart.

for the Octoson by analyzing echoes of random scatter from a sample volume positioned at different distances from the transducers and were typically small (<20%), since the range of analyzed tissue was small (4–5 cm) compared to the long focal length of the transducers (35 cm). The corrected curves were fit to exponential functions using least-squares error analysis to determine the magnitude of attenuation at 15 discrete frequencies between 2 and 3 MHz. Agreement between the two scans was ±10% at each frequency, demonstrating the reproducibility of the technique. The two estimates of attenuation were averaged together at each frequency, and a power law fit was performed to ascertain frequency dependence in each case.

RESULTS

A power law fit was found to provide a useful description of the magnitude and frequency dependence of attenuation values between 2 and 3 MHz. This is expressed mathematically as

$$\alpha = \alpha_0 f^n \qquad (1)$$

where α is attenuation in dB/cm, f is frequency in MHz, and α_0 and n are constants which characterize magnitude and frequency dependence, respectively. The correlation coefficient r, a measure of the match between measured attenuation values and the power law fit, was found to be greater than 0.9 in all cases (TABLE I).

Of the 10 normal subjects studied, 8 were found to exhibit a nearly linear curve of attenuation *vs.* frequency (n = 1); values of α_0 clustered around 0.5 dB/cm-MHz, close to the attenuation of fresh beef liver (9). The other 2 normal subjects had significantly higher attenuation, with a frequency dependence of less than 1, while the boy with focal nodular hyperplasia had the highest value (n = 1.46). Overall, magnitude (α_0) ranged between 0.33 and 1.05 dB/cm-(MHz)^n, while frequency dependence (n) varied from 0.56 to 1.46.

DISCUSSION

A useful format for interpretation of the results is a graph of attenuation ÷ frequency *vs.* frequency. Dividing attenuation by frequency normalizes the data, reducing the scale over which the values extend and facilitating visual estimation of frequency dependence. Thus if attenuation α(dB/cm) increases linearly with frequency, as is commonly assumed to be the case for normal liver (4, 5), then attenuation can be expressed mathematically as

$$\alpha = \beta \cdot f \qquad (2)$$

where β (dB/cm-MHz) is the slope or coefficient of attenuation for that tissue. Under these conditions, the graph would show a horizontal line (Fig. 2, a). However, if attenuation measured over a range of frequencies can be described more accurately by a power law curve, then the mathematical description is given by Equation 1. In this more general case, two parameters are now required for tissue characterization: α_0, which is the magnitude of attenuation at 1 MHz, and power law dependence which is represented by n. For the special case where n = 1, Equation 1 reduces to Equation 2; α_0 is equal to β and a horizontal line would result as noted above. If attenuation follows power law dependence over the frequency range of interest and n is greater than 1, then the slope will be positive; while if n is less than 1, the curve will slope downward (Fig. 2, b).

Figure 3 gives measured attenuation/frequency values for 2 normal subjects (CASES II and III) who are representative of 8 persons in our series. The slope of the normalized attenuation curve is nearly horizontal, indicating that n is equal to 1 and the relationship between frequency and attenuation is almost linear. In contrast,

Figure 4

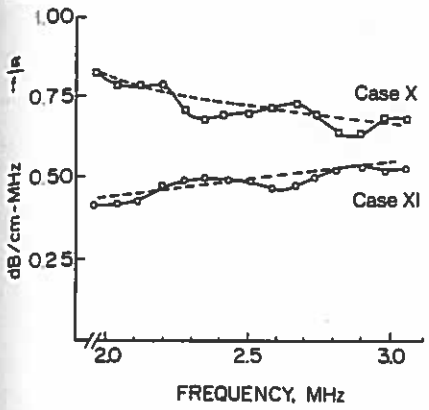

Measured values of attenuation ÷ frequency for two subjects with values of n significantly less than (CASE X) or greater than 1 (CASE XI). Solid lines = measured attenuation values; dotted lines = power law curve fit using the parameters given in TABLE I.

Figure 5

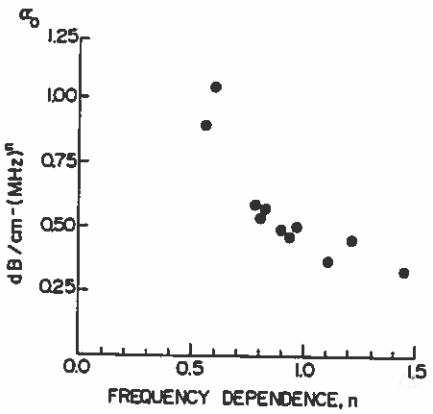

Plot of α_0 against n for all 11 subjects. The standard deviation of the value represented by each data point is approximately 20% in both dimensions.

Figure 6

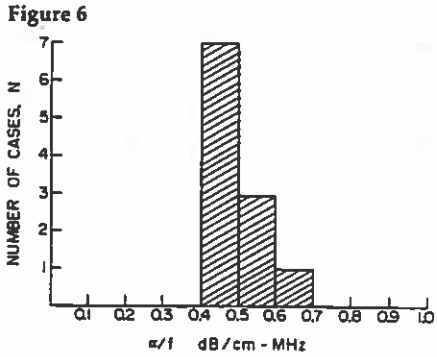

Bar graph representing the same 11 subjects but with no allowance for frequency dependence. Distinction between groups is reduced compared to Figure 5, which takes into consideration frequency dependence as well as magnitude.

the patients shown in Figure 4 have values of n which are significantly different from 1.0. The boy with focal nodular hyperplasia of the liver (CASE XI) had the highest value, $n = 1.46$. It has been demonstrated that increased collagen content can heighten ultrasonic attenuation in tissue (10, 11), which could contribute to the higher frequency dependence measured in this case. Two presumably normal subjects (CASES IX and X) were found to have n values of 0.56 and 0.60, respectively: however, visual inspection of the scan showed no evidence of abnormality, and thus the reason for the low value of n is not known. Theoretically, such a change in frequency dependence could be linked to a shift in the distribution of relaxational time constants (12); however, evaluation of the underlying mechanism will require further studies.

Values of α_0 and n are plotted against each other for all 11 subjects in Figure 5. The patient with confirmed liver abnormality (CASE XI) is clearly separable from the other subjects, having a lower value of α_0 but a higher value of n than the normal individuals. Most of the normal subjects are clustered around $\alpha_0 = 0.5$ dB/cm-MHz and $n = 1.0$, while the 2 atypical cases are characterized by a high α_0 and $n < 1$ and also occupy a clearly distinct region of the graph. Of course, power law values for n are sensitive to fluctuations in magnitude. For this analysis, a measured standard deviation of ±10% in attenuation magnitude at each frequency produced an uncertainty of about ±20% in estimates of α_0 and n for each case, which could be reduced still further by more extensive data averaging, *e.g.*, selecting larger regions for analysis or obtaining independent scan lines through the same region by varying the angle of incidence.

Present system accuracy is sufficient to separate our 11 cases into distinct groups when presented as a function of both α_0 and n, as shown in Figure 5. In contrast, if one were restricted to measuring only the magnitude of attenuation, the distinction between cases would be less clear. Figure 6 shows a bar graph representing the present study population, plotted as a function of attenuation at 3 MHz ÷ frequency; the range of attenuation values is similar to that covered in Figure 5, but without allowance for frequency dependence. It can be seen from Figure 6 that the separation of values is not as distinct when magnitude alone is presented. Thus it is apparent that calculation of frequency dependence is of value not only in terms of improved theoretical understanding of attenuation mechanisms in tissue, but also as a means of discriminating between different types of abnormalities.

CONCLUSIONS

Our measurement technique has been shown to be accurate since it correctly determined the attenuation coefficients of tissue-simulating phantoms used as reference standards (3). In this study, measurements of attenuation were both consistent and reproducible from one scan to the next within the same individual. The results we obtained with our liver samples are important for three reasons. The fact that the frequency dependence of attenuation differed significantly from the expected linear relationship indicates that an analysis which assumes such linear behavior *a priori* cannot be applied to all situations. It is also apparent that a multivariate approach to tissue characterization which makes use of both attenuation magnitude and frequency dependence information permits a more distinct separation of cases than either magnitude alone or visual inspection of the scans. Finally, since representative values of magnitude and frequency dependence are essential for development of theoretical tissue models representing both normal and pathological conditions, we feel that our measurements should increase one's understanding of diagnostic ultrasound. Further studies extending such measurements to include additional pathological conditions in the liver and other organs seem warranted, with emphasis on the dependence of accuracy on beam width, pulse length, time windows, and tissue backscatter statistics.

Acknowledgments: We would like to thank Raymond Gramiak, M.D. for his helpful suggestions and Bonnie A. Maye for her assistance in signal processing.

Department of Electrical Engineering
University of Rochester
Rochester, N.Y. 14627

References

1. Lele PP, Namery J. A computer-based ultrasonic system for the detection and mapping of myocardial infarcts. Proc IEEE 1974; 13:121–132.
2. Mimbs JW, O'Donnell M, Miller JG, Sobel BE. Changes in ultrasonic attenuation indicative of early myocardial ischemic injury. Am J Physiol 1979; 236:H340–H344.
3. Parker KJ, Waag RC. Measurement of ultrasonic attenuation within regions selected from B-scan images. IEEE Trans Biomed Eng 1983; 30:431–437.
4. Kuc R. Clinical application of an ultrasound attenuation coefficient estimation technique for liver pathology characterization. IEEE Trans Biomed Eng 1980; 27:312–319.

5. Flax SW, Pelc NJ, Glover GH, Gutmann FD, McLachlan M. Spectral characterization and attenuation measurements in ultrasound. Ultrasonic Imaging 1983; 5:95–116.
6. Fellingham LL, Stern RA, Gamboa-Aldeco A, Solomon H, Sommer FG. Ultrasonic characterization of normal and diffusely diseased liver (abst). J Ultrasound Med 1983; 2 (Suppl):162.
7. Narayana PA, Ophir J. On the validity of the linear approximation in the parametric measurement of attenuation in tissues. Ultrasound Med Biol 1983; 9:357–361.
8. Harris FJ. On the use of windows for harmonic analysis with the discrete Fourier transform. Proc IEEE 1978; 66:51–83.
9. Parker KJ. Ultrasonic attenuation and absorption in liver tissue. Ultrasound Med Biol 1983; 9:363–369.
10. Goss SA, Frizzell LA, Dunn F, Dines KA. Dependence of the ultrasonic properties of biological tissue on constituent proteins. J Acoust Soc Am 1980; 67:1041–1044.
11. O'Donnell M, Mimbs JW, Miller JG. Relationship between collagen and ultrasonic backscatter in myocardial tissue. J Acoust Soc Am 1981; 69:580–588.
12. Pauly H, Schwan HP. Mechanism of absorption of ultrasound in liver tissue. J Acoust Soc Am 1971; 50:692–699.